83-2657

OPTICAL EFFECTS OF SPACECRAFT-ENVIRONMENT INTERACTION: SPECTROMETRIC OBSERVATIONS BY THE DE-B SATELLITE

Vincent J. Abreu, Wilbert R. Skinner, and Paul B. Hays
Space Physics Research Laboratory
The University of Michigan
Ann Arbor, Michigan 48109

Jeng-Hwa Yee
Harvard-Smithsonian Center for Astrophysics
Cambridge, Massachusetts 02138

Abstract

Data from the Fabry-Perot interferometer on board the Dynamics Explorer-B satellite is used to show that the contaminant glow observed by Yee and Abreu at 7320Å on the AE satellites is produced by emission lines of one or more species. A comparison is made of the contaminant spectrum near 7320Å with the nightglow OH spectrum measured below 155 km. Evidence is presented to the effect that OH might be one of the metastable species producing the glow.

I. Introduction

The characteristics and spectral variation of the optical glow induced by spacecraft-atmosphere interaction have been recently described by Yee and Abreu [1982, 1983] using photometric data obtained by the Visible Airglow Experiment (VAE) on board the Atmosphere Explorer satellites [Hays et al., 19731. Their data showed that: 1) the most intense radiation comes from surfaces facing the direction of motion of the satellite; 2) the contamination has a band or continuum spectrum which is brighter toward the red; and 3) there is a strong correlation between emission intensity and oxygen atom density in the 160-280 km altitude range. Yee and Abreu suggested that the glow is produced by molecules which are formed and ejected from the satellite surface in a metastable state after surface particles undergo chemical reaction or direct impact collisions with incoming $O(^3P)$ atoms at the satellite velocity ($\sim$8 km sec^{-1}). Later, based on the apparent spectral distribution and the radiative lifetime deduced by Yee and Abreu ($\sim$5 msec) Slanger [1983] showed that the OH Meinel bands are a tenable identification for the AE satellite glow. He proposed that OH is produced by the interaction of 5 ev $O(^3P)$ atoms and adsorbed water and/or C-Hbonds in the satellite construction material. So far, however, no spectroscopic measurements have been reported which confirm this hypothesis.

The Dynamic Explorer-B spacecraft is a modified version of the Atmosphere Explorer spacecrafts, whose payload included a high resolution Fabry-Perot interferometer (FPI) designed to measure temperatures and winds in the thermosphere. Given the similarity between the spacecrafts, we have used high resolution data obtained by the FPI in a spectral region centered around 7320Å in order to provide further evidence concerning the nature of the processes producing the optical glow. The spectral region to be investigated corresponds to the 8-3 OH emission band. This emission is also very strong in the terrestrial nightglow producing a narrow emission layer which peaks in the upper mesosphere. Consequently, a comparison of spectra obtained at mesospheric heights with those obtained at satellite altitudes ($\sim$250 km) should provide the necessary information to show whether OH is one of the emitting metastable species producing the optical glow. This analysis is presented in this paper.

II. Description of Instrument

The Fabry-Perot interferometer on Dynamics Explorer-B is a remote sensing instrument designed mainly to measure the temperature, meridional wind and density of metastable $O(^1S)$ and $O(^1D)$ atoms and the $O^+(^2P)$ ion in the thermosphere. A detailed description of the instrument has been given by Hays et al. [1981], Killeen et al. [1983], and Killeen and Hays [1983].

The measurements are made with a high resolution Fabry-Perot etalon, which performs a wavelength analysis on light detected from atmospheric emission features by spatially scanning the interference fringe plane with 12 concentric ring detectors. The scan is linear in wavelength, covering a spectral range equal to 0.01796Å per detector channel at 7320Å. The number of free spectral ranges focused on the detector is 1.0135 at this wavelength. The spectral region for analysis was selected by a 10Å halfwidth interference filter centered at 7320Å. The etalon and detector parameters of interest are summarized in Table 1.

Table 1 Parameters of Interferometer

1. Free Spectral range	0.212651 (7320Å)
2. Fraction of the free spectral range on detector	1.0135 (7320Å)
3. Detector anode structure	12 concentric rings equal area anodes
4. Spectral range per anode	0.01796; (7320Å)

A sequential altitude scan performed by a commandable horizon scan mirror provides the spatial information at sixteen tangent heights below the orbit of the satellite. Figure 1 is a schematic which shows the detector position relative to the velocity vector of the spacecraft, as well as the range of tangent altitudes scanned by the mirror. The altitude scan was limited to the angular region from 5 to 15 degrees below the local horizon, with a field of view of 0.9 degrees (half-cone angle).

The sensitivity of the instrument was determined in a pre-flight calibration to be .04 counts/Rayleigh-sec. For this analysis the sensitivity was also determined by an in-flight calibration using the daytime thermospheric $O^+(^2P)$ emission at 7319.079A and 7320.1548. The production and loss processes, as well as the reaction rates involved in the calculation of the volume emission rate of this emission are well known. The sensitivity was then estimated from a theoretical calculation of the brightness [Abreu et al., 19801 and simultaneous

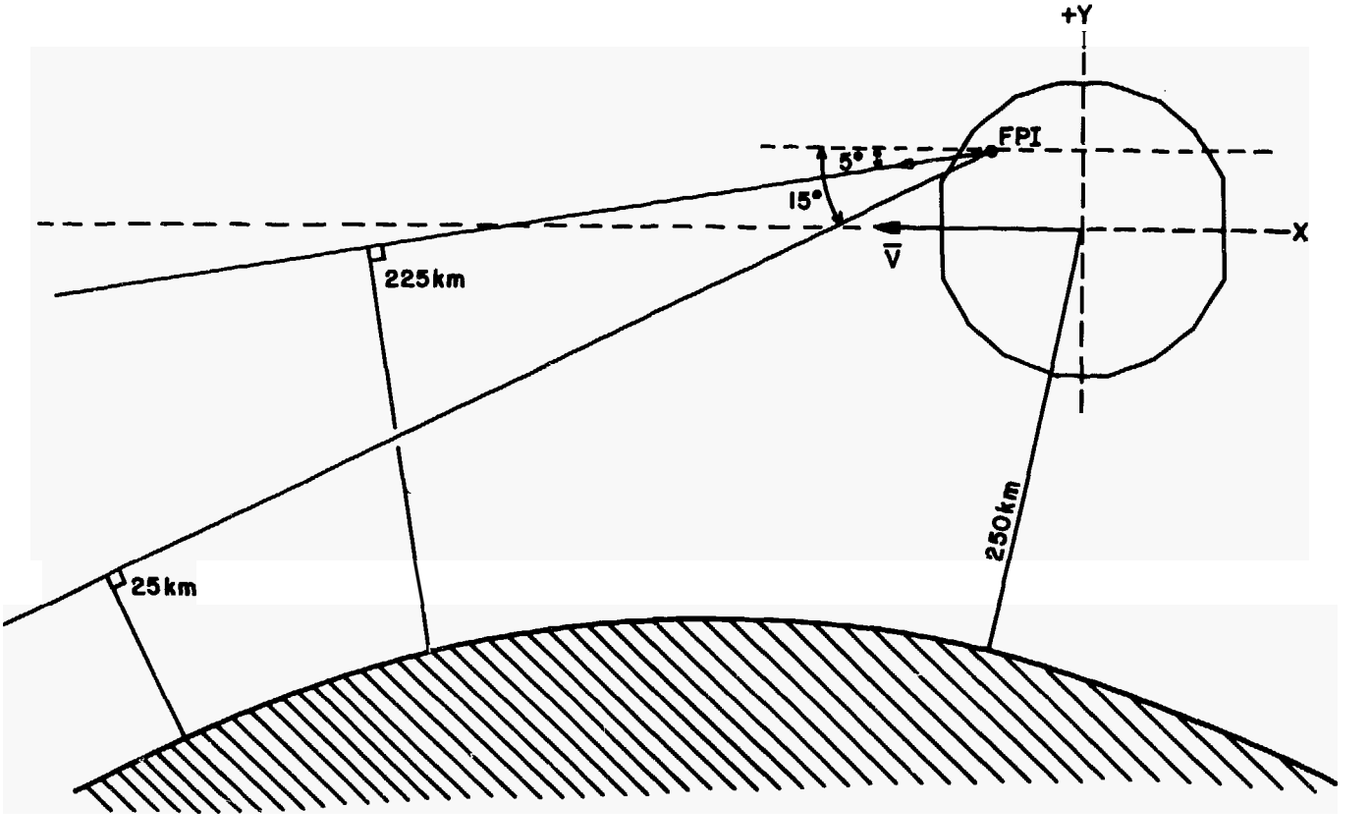

Figure 1 Schematic showing the detector position relative to the velocity vector of the spacecraft, as well as the range of tangent altitudes scanned by the mirror.

measurements of the Fabry–Perot detector counts, the thermospheric temperature and the O and N_2 densities made at the satellite altitude. Both calibrations are in good agreement.

For illustrative purposes, Figure 2 shows a spectrum of the $O^+(^2P)$ emission at 7319.079Å and 7320.1541. The units in the vertical axis are counts/integration period (I-P.). One integration period equals 0.22 sec. Since the transfer function of the Fabry–Perot is periodic, the relative position of the two lines in the image plane detector depends on $\Delta\lambda/FSR$, where AA is the wavelength separation between the two lines and FSR is the free spectral range of the etalon. The channel separation (number of channels apart) in the image plane detector is given by

$$\left(\frac{\Delta\lambda}{FSR} - INT(\Delta\lambda/FSR)\right) \cdot FSR/\delta\lambda$$

where INT represents the integer part of the argument and $\delta\lambda$ is the spectral range of a ring. The doublet under consideration is .65 channels apart. Consequently, the two lines appear superimposed as a single line centered on channel 6. The width of the line corresponds to a temperature of ~1000°K.

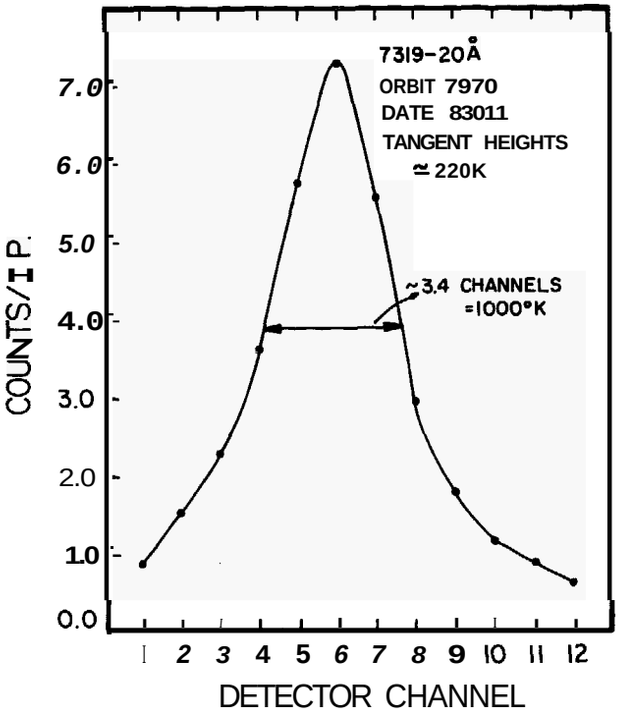

Figure 2 Spectrum of the $O^+(^2P)$ emission obtained during the daytime.

III. Data Analysis

We have chosen for this study spectra measured by the FPI at tangent heights between 60 and 225 km. These spectra were obtained while the spacecraft was near perigee (~250 km) and in a despun mode. Data were rejected if the solar zenith angle at the tangent point or at the satellite location was less than 130 degrees, and if the absolute value of the

tic latitude was greater than 55 degrees at the sateilite location. If the satellite was moving polcward data were rejected if the absolute value of the magnetic iatitude was greater than 40 degrees at the tangent height. The above constraints insured that data were not contaminated by daytime or high latitude auroralemissions.

The most prominent feature in the spectral range of interest (7320Å ± 10Å) in the night airglow are the vibration - rotation transitions in the ground electronic level of OH. The excitation process for this emission is generally assigned to the reaction

$$H + O_3 \rightarrow OH(X^2\Pi, v) + O_2$$

[Bates and Nicolet, 19501. In general, the OH emission occurs in a thin layer which peaks around 90 km. The width of the layer is of the order of 10 km at half-intensity [Watanabe et al., 19811. Based on the morphology of the nightglow just presented, one would expect the observed spectrabelow 155 km to be that of OH, while those above 155 km to be the spectra of the contaminant glow. This hypothesis will be investigated further in this analysis.

A. The Contaminant Glow Spectrum

A spectrum of the emission above 155 km has been obtained by averaging approximately 6000 nighttime spectra with tangent heights up to ∿ 225 km. The average satellite altitude was 253 km. The spectrum is presented in Figure 3. The spectra had an estimated dark count removed and were normalized to remove interchannel sensitivity differences. The negative counts shown in Figure 3 are due to an imperfect knowledge of the dark count.

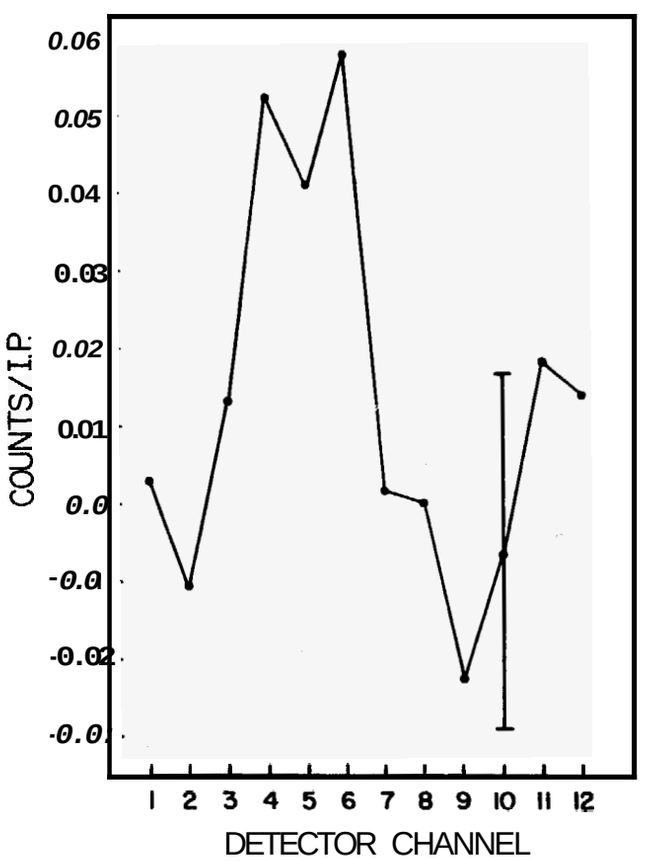

Figure 3 Spectrum of the contaminant glow.

One may wonder if the observed spectrum is that of the contaminant glow or if it is instead the spectrum of the nightglow in the thermosphere. Evidence that it is the former is provided by the fact that the same spectral shape and intensities are observed at all mirror positions with tangent heights above 155 km. Further proof is provided by comparing the photometric intensity observed here with the 7319-20Å brightness of the glow observed at 250 km by Yee and Abreu [1981] using data from the VAE photometers on the Atmosphere Explorer satellites. The photometric brightness is obtained by adding the counts from each detector and multiplying the resulting counts by the calibration factor. The brightness thus obtained is ∿20 Rayleighs. This is in good agreement with the 7319-20Å contaminant emission observed at 250 km by Yee and Abreu. Consequently, we conclude that the spectrum observed above 155 km by the Fabry-Perot interferometer is that of the contaminant glow, and that the photometric brightness observed by Yee and Abreu on the AE satellites is not a continuum, but is produced by the emission lines of one or more species which remain to be identified. For this purpose we will next consider the OH spectra measured below 155 km.

B. OH Spectra

Figure 4 shows OH spectra at different tangent heights obtained during orbit 8058. The intensity of each spectrum as a function of altitude is consistent with the presence of a narrow layer which peaks at ∿80 km. Below this altitude the spectra consists of two distinct emission lines which peak on channels 4 and 9, respectively. Above 80 km, the two lines come closer and they seem to converge at approximately 92 km. The apparent convergence of the two lines is due to a field of view effect, which comes about when the thin emission layer is viewed from above by the 12 channel detector. Under these circumstances each channel in the detector has a different field of view. The different intensities observed by the detector channels cause the distortion observed in the spectra. The distortions are greater in the outer channels of the detector. In order to correct the spectra it is necessary to effect a deconvolution for each detector channel, of the signal as a function of altitude with the field of view of the particular channel. The large uncertainties in the data, however, limit the accuracy of the inversion process and the recovered spectra are not free of distortions. We have effected the deconvolution of the spectra shown in Figure 4 and have averaged the spectra from tangent heights equal to 62, 72 and 82 km, after being normalized to their respective photometric brightness (area). The resultant spectrum is shown in Figure 5. Spectra from the topside of the emission layer were not averaged because the effect of the field of view is most significant in that region. It should be noted that the separation between the two spectral lines observed is approximately 5 channels. Laboratory measurements of the 8-3 band of OH have identified two lines at 7318.268Å and 7318.337Å [Coxon and Foster, 19821. These two lines would appear 4 channels apart on the FPI detector, so there is a high probability that these are the two emission lines observed here. The absolute wavelengths of these two lines are not known to the accuracy necessary to predict their relative position to the $O^+(^2P)$ 7320Å line on the FPI detector.

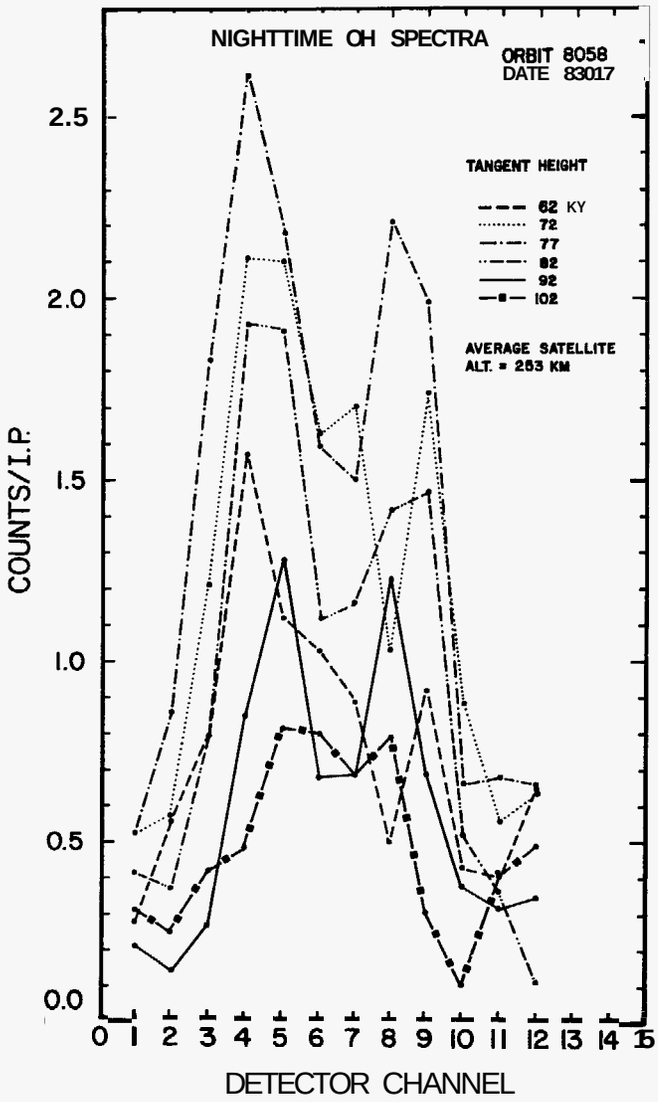

Figure 4 OH spectra at different tangent height.

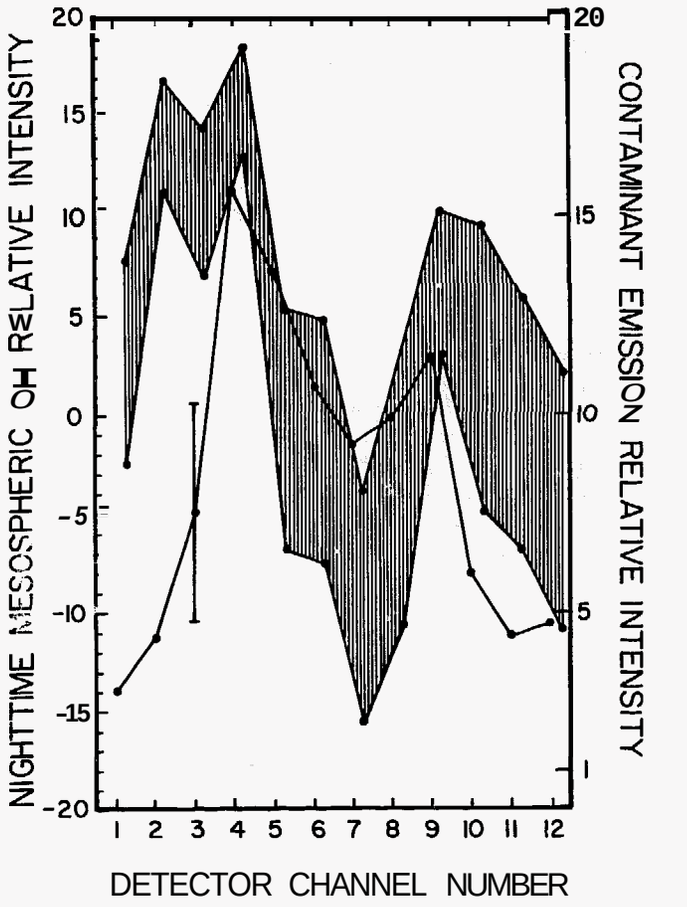

Figure 5 A comparison of the OH nightglow and the contaminant glow spectrum. The contaminant glow spectrum has been shifted by the component of the satellite velocity along the line of sight.

The contamination spectrum, normalized to the photometric brightness is also shown in Figure 5. The shaded area indicates the statistical uncertainty in the measurements. Since the OH emission spectrum is doppler shifted by the component of the satellite velocity (∿7.8 km/sec) along the line of sight, we have shifted the contamination spectrum by the same amount for comparison purposes.

The shape of the contaminant spectrum from channels 4 through 12 agrees well with that of the OH spectrum. This fact lends confidence to the hypothesis that OH is the contaminant species. The contaminant spectrum, however, suggests an additional peak on channel 2 which is not present on the nightglow OH spectrum. This could be another OH line or an emission line from other species. Although we have not definitely proven that OH is one of the species producing the glow, the data presented here do provide some evidence to this effect. One should be careful not to transfer these results directly to the interpretation of the glow observed in the Shuttle, since different types of contaminants are present in the Shuttle environment.

IV. Conclusion

Data from the Fabry-Perot interferometer on board the DE-B satellite have been used to show that the contaminant glow observed by Yee and Abreu at 7320Å on the AE satellites is produced by emission lines of one or more species. A comparison of the contaminant spectrum near 7320Å with the nightglow OH spectrum obtained below 155 km has provided evidence to the effect that OH might be one of the species producing the glow.

References

Abreu, V. J., W.R. Skinner, and P.B. Hays, Airglow measurements of the variation of the $O^+(^2P)$ ionization frequency during solar cycle 21, Geophys. Res. Lett., 7, 109, 1980.

Bates, D.R., and M. Nicolet, The photochemistry of Atmospheric water vapor, J. Geophys. Res., 55, 301. 1950.

Coxon, J.A., and S.C. Foster, Rotational analysis of hydroxyl vibration-rotation emission bands: Molecular constants for OH $X^2\Pi$, $6 \leq v \leq 10$, Can. J. Phys., 60, 41, 1982.

Hays, P.B., G.R. Carignan, B.C. Kennedy, G.G. Shepherd, and J.C.G. Walker, The visible airglow experiment on Atmosphere Explorer, Radio Sci., 8, 369, 1973.

Hays, P.B., T.L. Killeen, and B.C. Kennedy, The Fabry-Perot interferometer on Dynamics Explorer, Space Sci. Instr., 5, 395, 1981.

Killeen, T.L., B.C. Kennedy, P.B. Hays, D.A. Symanow, and D.H. Checkowski, An image plane detector for the Fabry-Perot interferometer on Dynamics Explorer, Appl. Opt., accepted for publication, August 1983.

Killeen, T.L., and P.B. Hays, Doppler line profile analysis for a multi-channel Fabry-Perot Interferometer, to be sumbitted to Appl. Opt., 1983.

Slanger, T.G., Conjectures on the origin of the surface glow of space behicles, Geophys. Res. Lett., 10, 130, 1983.

Watanabe, T., M. Nakamura, and T. Ogawa, Rocket measurements of O_2 atmospheric and OH Meinel bands in the airglow, J. Geophys. Res., 86, 5768, 1981.

Yee, J.H., and V. J. Abreu, Optical contamination on the Atmosphere Explorer-E satellite, Proceedings of SPIE Technical Symposium, , 120, 1982b.

Yee, J.H., and V. J. Abreu, Visible glow induced by spacecraft-environment interaction, Geophys. Res. Lett., 10, 126, 1983.

Acknowledgment

This work was supported by NASA grant number NAS5-25691.

END